Oceanologia (2020) 62, 1—11

Available online at www.sciencedirect.com

ScienceDirect

journal homepage: www.journals.elsevier.com/oceanologia

ORIGINAL RESEARCH ARTICLE

Hydrogeochemistry and magnitude of SGD in the Bay of Puck, southern Baltic Sea

Żaneta Kłostowska[a], Beata Szymczycha[a,*], Monika Lengier[a], Dorota Zarzeczańska[b], Lidia Dzierzbicka-Głowacka[a]

[a] *Institute of Oceanology, Polish Academy of Sciences, Sopot, Poland*
[b] *Faculty of Chemistry, University of Gdańsk, Gdańsk, Poland*

Received 2 July 2019; accepted 12 September 2019
Available online 26 September 2019

KEYWORDS
Subterranean estuary;
Groundwater discharge;
Macro ions

Summary This work reports the hydrogeochemistry of submarine groundwater discharge (SGD) in the Bay of Puck, southern Baltic Sea. To understand the seasonal and spatial variability of SGD, groundwater and seawater-based SGD samples were collected in several sites in November 2017, March 2018, May 2018 and July 2018. Additionally, a vertical, one-dimensional, advection-diffusion model was used to estimate SGD in each site. The obtained results ranged from to 1.8×10^{-7} L cm^{-2} s^{-1} to 2.8×10^{-7} L cm^{-2} s^{-1} and depended on both: short-timescale factors (wind direction and monthly precipitation) and long-timescale factors (total precipitation and large-scale sea level variations). The calculated rates were further extrapolated to the entire Bay of Puck and ranged from 16.0 m^3 s^{-1} to 127.7 m^3 s^{-1}. The estimated SGD fluxes were significantly higher than results including only the freshwater component of SGD. In the Baltic Sea the importance of SGD, as a source of water and accompanying chemical substances, is still neglected, however, the present findings indicate that locally SGD can be higher than rivers runoff.

1. Introduction

Submarine groundwater discharge (SGD) is defined as all flow of water coming from the seabed to the water column, regardless of the fluid composition or driving force (Burnett et al., 2003). It includes both fresh groundwater discharge derived from terrestrial recharge and recirculated seawater (Burnett et al., 2006). In ocean research, any subsurface water is considered to be groundwater, but traditional hydrogeologists reserve the term groundwater for the

* Corresponding author at: Institute of Oceanology, Polish Academy of Sciences, ul. Powstańców Warszawy 55, 81—712 Sopot, Poland, Tel.:+48587311738; fax +48585512130.
E-mail address: beat.sz@iopan.gda.pl (B. Szymczycha).
Peer review under the responsibility of Institute of Oceanology of the Polish Academy of Sciences.

Production and hosting by Elsevier

https://doi.org/10.1016/j.oceano.2019.09.001

water that originates from a terrestrial aquifer, which excludes recirculated seawater (Jiao and Post, 2019). This difference in terminology has caused the misunderstanding when SGD is estimated by different methods. It is worth mentioning, that the total SGD (including fresh and recirculated water) tends to be much higher than fresh SGD and can be comparable to river flux (Moore, 2010). In this study, the term SGD is used for both fresh SGD and recirculated SGD.

For many decades SGD was neglected in the global hydrological cycles. The reason for that is the difficulty to identify and measure SGD. Generally, rivers have been recognized to be a key pathway for terrestrial water to the ocean. Since Moore (1996) showed that chemical mass flux via SGD can exhibit 40% of this coming from the river water the subject has been receiving increased attention. SGD can be an important source of chemical substances as aquifers in many areas become enriched with chemicals (organic and inorganic substances) from land sources. Consequently, SGD should be considered in analyzing the chemical substances' budgets of coastal ecosystems.

Recently, several geochemical processes occurring in the groundwater-seawater mixing zone, such as precipitation/dissolution of ion, speciation of trace metals, the removal of nutrients, and the production of dissolved inorganic carbon (DIC) have been identified as modifying the chemical substances' fluxes via SGD (Cai et al., 2003; Charette and Sholkovitz, 2002, 2006; Kroeger et al., 2007). Relatively less attention has been attributed to the macro ions' (Cl^-, SO_4^{2-}, Na^+, K^+, Mg^{2+}, Ca^{2+}, and HCO_3^-) cycling, even though major ion distributions due to groundwater discharge can exert a much control over the chemical functioning of the coastal area (Liu et al., 2017; Santos et al., 2008).

In the Bay of Puck, southern Baltic Sea preliminary studies indicated that locally SGD is an important component of chemical budgets (e.g., Bolałek, 1992; Pempkowiak et al., 2010; Piekarek-Jankowska, 1994; Szymczycha et al., 2012, 2014, 2016). However, little is known about the SGD hydrogeochemistry, its magnitude, and variability. In this study, we investigated the hydrogeochemical characteristics and related hydrogeochemical processes. We sampled both the shallow groundwater wells (piezometers) and offshore SGD (pore water) in order to understand the dynamic character in the transition zone (subterranean estuary). Moreover, a vertical, one-dimensional, advection-diffusion model was used to estimate SGD. The obtained results were extrapolated to the entire bay assuming similar SGD rates in the area of comparable pore water salinity and knowing the literature SGD coverage in the Bay of Puck (Piekarek-Jankowska, 1996, 1996; Kozerski (Ed.), 2007; Kryza and Kryza, 2006). Additionally, SGD was correlated to both the short-timescale factors (wind direction and precipitation) and the long-timescale factors (large-scale sea level variations).

2. Material and methods

2.1. Study area

The Bay of Puck is an inner part of the Bay of Gdańsk and is an example of an active groundwater discharge area (Bolałek, 1992; Pempkowiak et al., 2010; Piekarek-Jankowska, 1994; Szymczycha et al., 2012, 2014, 2016). It is divided into two parts, the outer part with an average depth of 21 m and the inner, shallower part reaching a depth of about 3 m (Urbański et al., 2007). Hence, the inner part of the bay has limited access to the open Baltic Sea waters due to a natural barrier called Rybitwia Mielizna (Urbański et al., 2007), while the whole bay is separated by a narrow spit, called Hel Peninsula, from the open Baltic Sea (Nowacki, 1993).

The bay's hydrological regime is controlled by the exchange of mass, energy, and outflow from its catchment area, while the outer part of the bay is further influenced by contact with the Gulf of Gdańsk and the Vistula River (Cyberski, 1993). Both bays, namely the Bay of Puck and the Gulf of Gdańsk, have complex, hydrological systems consisting of Cretaceous, Tertiary, and Quaternary aquifers (Kozerski (Ed.), 2007). The detailed hydrogeological characteristics and drainage zones of the fresh groundwater in the Bay of Puck were presented by Piekarek-Jankowska (1996). In the Supplementary Material Figure 1S, the cross-section presenting the hydrogeological conditions of the sediments of the Bay of Puck is presented while in the Supplementary Material Figure 2S the SGD discharge zones modified after Piekarek-Jankowska (1994) and Kryza et al. (2005) are indicated.

The lithological characteristic of the Bay of Puck is closely related to the lagoon bay type. Generally, the grain size increases with the distance from the shoreline, which correlates with the depth and morphology of the bay (Piekarek-Jankowska, 1994). In the inner part of the bay, a small diversity of bottom sediments is observed. They are mainly dominated by fine-grained sands; however the coastal zone, until the 1 m isobath, is formed by medium-grained sands. In the outer part of the bay, the proportion of mud and clay increases according to the lithological diversity of the sediments (Piekarek-Jankowska and Łęczyński, 1993; Uścinowicz and Kramarska, 2011). The coarse-grained sands dominate to a depth of about 20 m, while the fine-aurantite sands are the majority in the deepest parts. The bay also contains a variety of shore types (e.g., sandy beaches, gravel beds, stony outcrops, clay cliffs, and vegetated river mouths).

2.2. Sampling and analytical procedures

SGD, shallow groundwater and seawater samples were collected in November 2017, March 2018, May 2018 and July 2018. The coastal SGD sites were located off Hel Peninsula (Hel, Jastarnia, and Chałupy) and off the mainland (Swarzewo, Osłonino, and Puck). Two of them — Hel and Jastarnia — were located in the outer part of the bay, while the other sites were located in the inner part of the bay (Fig. 1).

SGD samples for macro ions composition were collected at 10 cm depths by means of push points (e.g., Szymczycha et al., 2012) every 1 m along a 5-m-long transect perpendicular to the shoreline at each study site. Additionally, pore water from several depths up to 30 cm was collected 3 m offshore for chloride analyses. In July 2018, at every coastal SGD site, salinity surveys were recorded along 10-m-long, parallel transects that extended 5 m seaward (Fig. 2). Pore

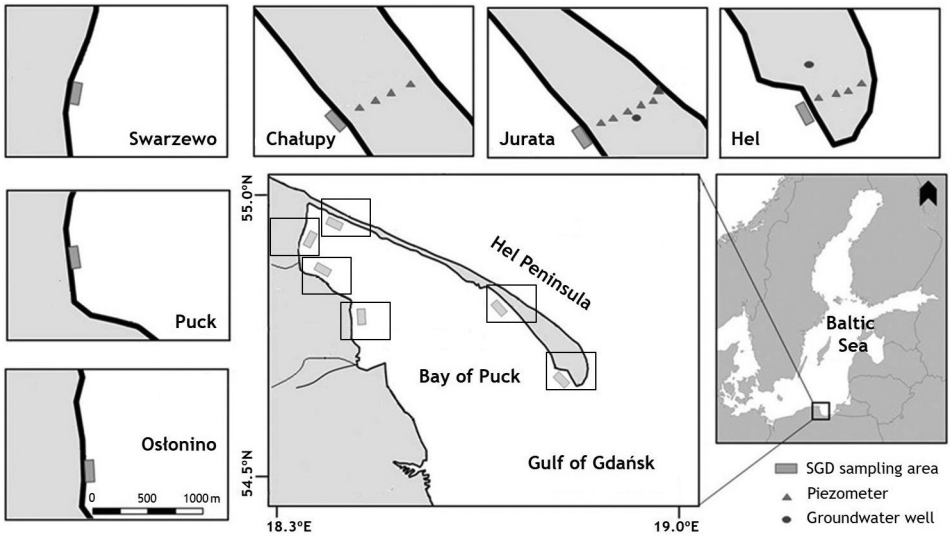

Figure 1 Map of the study sites located in the Bay of Puck, southern Baltic Sea. The submarine groundwater discharge (SGD) sites situated off Hel Peninsula (Hel, Jurata, Chałupy) and off the mainland (Puck, Swarzewo, and Osłonino) are marked as gray rectangles, while piezometers and groundwater wells are marked as triangles and circles, respectively.

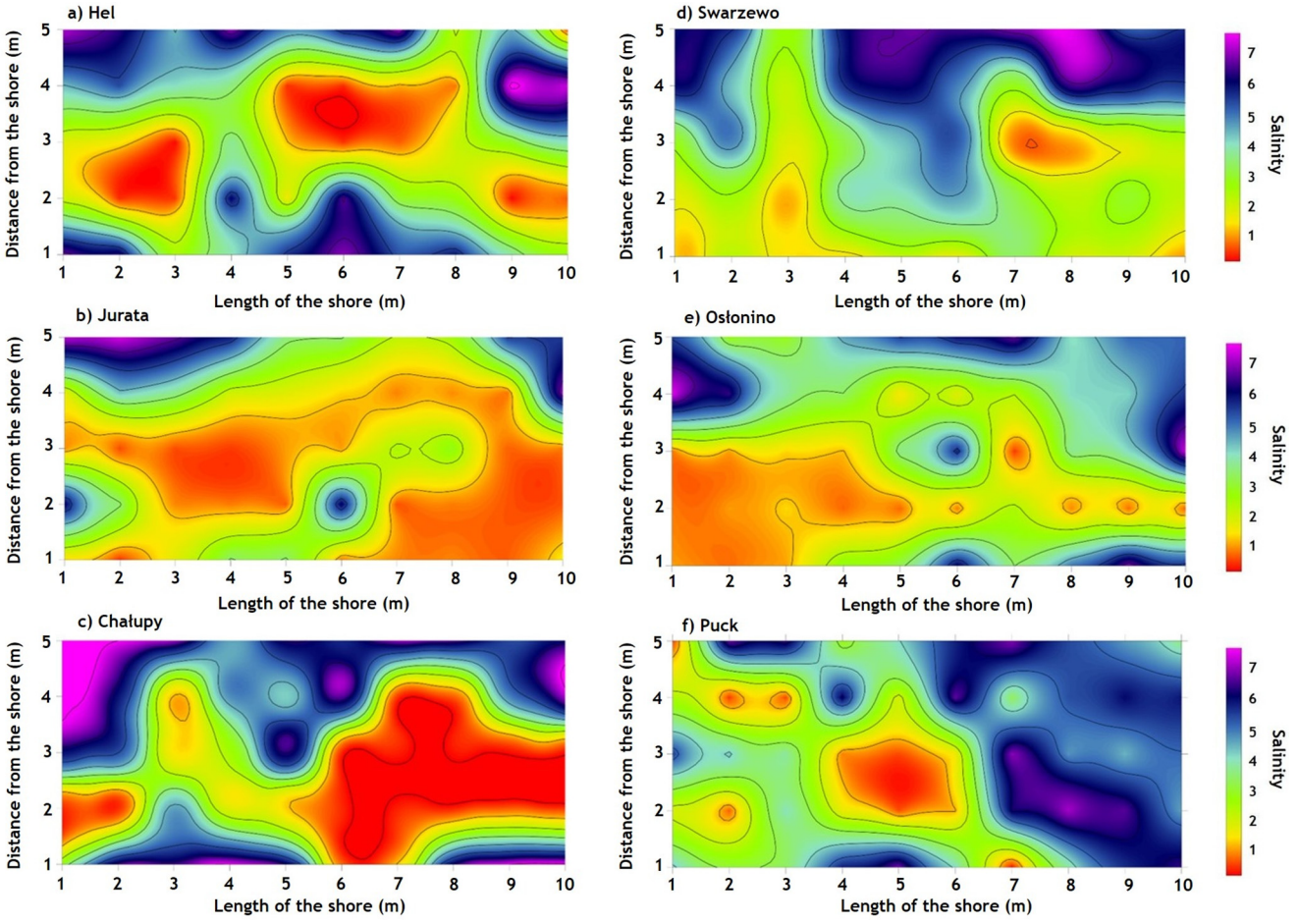

Figure 2 Porewater salinity distribution at 10 cm depth at six study sites located off Hel Peninsula — (a) Hel, (b) Jurata, (c) Chałupy — and off the mainland — (d) Swarzewo, (e) Osłonino, and (f) Puck — within the Bay of Puck, southern Baltic Sea.

water samples were collected every 1 m from 10 cm depth by means of push points. Data interpolation was performed in Surfer15 (Golden Software Partner).

Seawater samples were collected directly from the sea within the survey.

Shallow groundwater samples were collected from 14 piezometers situated at Hel Peninsula (Fig. 1). Water samples from the piezometers were collected using a peristaltic pump and a Teflon tube. The depths of the piezometers' mirrors were determined in situ using a hydrogeological whistle and meter, and they ranged from 1 m to 8.2 m.

Field parameters, such as oxygen concentration (O_2), pH, oxidation–reduction potential (ORP), and salinity, were measured in situ by means of a multimeter (Hach-Lange).

In all collected water samples, major ions (Ca^{2+}, Mg^{2+}, Na^+, K^+, Cl^-, SO_4^{2-}, and HCO_3^-) were analyzed. 10 ml of each water sample were collected for major metals (Na^+, Mg^{2+}, Ca^{2+}, and K^+) analyses. Samples were filtrated through cellulose acetate filters ($\varphi = 0.45\ \mu m$) into pre-prepared PE vials, preserved with 100 μL 3 M nitric acid (V) (HNO_3), and stored in the dark at 4C until analysis. The ion measurements were conducted by means of atomic absorption spectroscopy (SHIMADZU 6800). Background correction was applied with a deuterium lamp using a flame technique (flame: air – acetylene). Quality control was performed using certified reference material "ERM-CA-11b". The recovery was equal for Mg^{2+} to 96%, Ca^{2+} to 96%, K^+ to 103% and Na^+ to 105%, while the precision, described as the Relative Standard Deviation (RSD) of triplicate analyses, was not worse than 3%.

Water sample for Cl^- analysis was collected (with a volume of 40 ml) into polythene (PE) containers and stored in the dark at 4°C until analysis. The analyses were carried out via the potentiometric titration method, using the syringe microtitrator Cerko Lab System with an ion-selective chloride electrode (Schott Ag 6280). A standard solution of silver nitrate (0.1 M and 0.01 M) was used as a titrant, and portions $V = 0.041$ ml were dosed automatically. Quality control was performed using the standard curves. The precision, described as (RSD) of triplicate analyses, was not larger than 3%. The obtained concentrations of the procedural blank samples never exceeded 4% of concentrations measured in the actual samples.

Water samples (40 ml) for the analysis of HCO_3^- were collected into vials made of borosilicate glass, conserved with 150 μl of saturated $HgCl_2$ solution, and stored in the dark at 4°C until analysis. The analyses were carried out using the potentiometric method, by means of a pH electrode (Cerko Lab System potentiometric microtitrator). As the titrant, a standard solution of hydrochloric acid (HCl) (0.1 M and 0.01 M) was used, and portions $V = 0.041$ cm^3 were dosed automatically. Quality control was performed using the standard curves. The precision, described as the RSD of triplicate analyses, was not worse than 3%. The obtained concentrations of the procedural blank samples never exceeded 4% of the concentrations measured in the actual samples.

Around 40 ml of sample was collected for SO_4^{2-} analysis into PE containers and stored in the dark at 4°C until analysis. The analyses were carried out with a conductometric precipitation titration method, using a conductivity cell probe (Schott LF413T-id) with a multi-parameter ProLab2000 meter (Schott Instruments). As the titrant, a standard barium acetate $Ba(CH_3COO)_2$ solution (0.005 M) was used. The titrant was added to the test sample in portions of 0.1 cm^3 in continuous measurement of conductivity, as well as pH and temperature control. For each sample, curves were plotted in a $\kappa' = f(VBa(CH_3COO)_2)$. Quality control for sulfate analysis was performed using standard curves. The precision, described as the RSD of triplicate analyses, was not worse than 3%. The obtained concentrations of the procedural blank never exceeded 5% of concentrations measured in the actual samples.

2.3. Ionic deltas

The ionic delta is an important indicator determining the nature of the geochemical reactions between the solid phase and the liquid phase in the coastal zone. The ionic delta is used mainly in studies of both SGD and seawater intrusion (Bolałek, 1992; Liu et al., 2017). It describes the difference between the measured concentration ($m_{i,sample}$) of ion (i) and its theoretical concentration ($m_{i,mix}$) when freshwater and seawater mix conservatively (Appelo and Postma, 2005; Liu et al., 2017) and can be described as:

$$\Delta m_i = m_{i,sample} - m_{i,mix}. \quad (1)$$

The theoretical concentration ($m_{i,mix}$) can be expressed as:

$$m_{i,mix} = f_{sea} - m_{i,sea} + (1 - f_{sea}) m_{i,fresh}, \quad (2)$$

where $m_{i,sea}$ and $m_{i,fresh}$ are the concentrations of the seawater endmember and freshwater endmember, respectively, and f_{sea} is the fraction of seawater, which is usually calculated from Cl^- concentration in the water sample because of the conservative properties of the chloride ion. The fraction, based on Cl^-, is described as:

$$f_{sea} = \frac{m_{Cl^-,sample} - m_{Cl^-,fresh}}{m_{Cl^-,sea} - m_{Cl^-,fresh}}, \quad (3)$$

where $m_{Cl^-,sample}$ is the concentration of Cl^- in the sample; $m_{Cl^-,fresh}$ is the concentration of Cl^- in the freshwater endmember; and $m_{Cl^-,sea}$ is the Cl^- concentration in the seawater endmember.

2.4. Piper diagram

The Piper diagram is widely used in hydrochemical studies concerning the composition of groundwater – specifically its graphical classification and selection of the source of origin (Hounslow, 1995; Piper, 1994). In the Piper diagram, major ions are plotted as cation and anion percentages of milliequivalents in two base triangles. The total cations in meq dm^{-3}, and the total anions in meq dm^{-3} are set equal to 100%. The data points in the two triangles are then projected onto the diamond grid. The projection reveals certain useful properties of the total ion relationships. Every sample is represented by three data points – one in each triangle and one in the projection diamond grid. In this study, the Piper diagram was performed in the RockWare Software: AqQA.

2.5. Calculation of SGD rates

Chloride is used as an SGD tracer in marine environments, as it does not undergo either adsorption or chemical reactions.

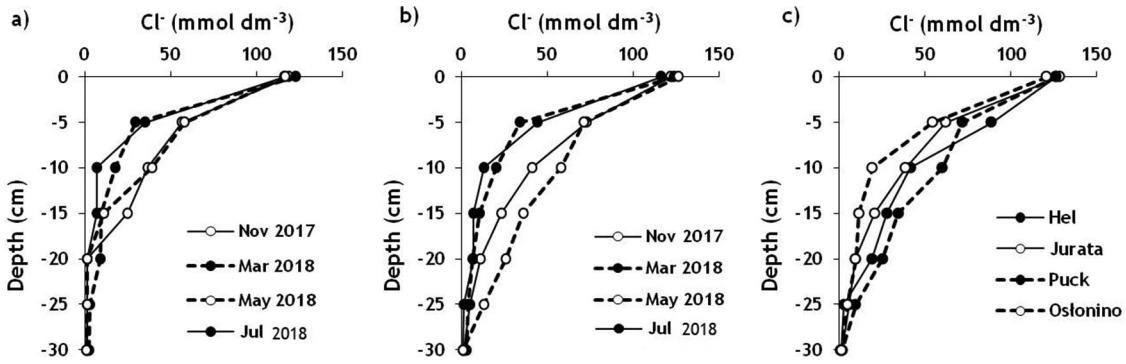

Figure 3 Seasonal pore water chloride (Cl^-) depth profiles for (a) Swarzewo, (b) Chałupy and (c) Hel, Jurata, Puck, and Osłonino collected in July 2018.

Therefore, pore water profiles of Cl^- solely reflect transport processes, such as advection and diffusion (Schlüter et al., 2004). The Cl^- pore water distribution can be described by a vertical, one-dimensional, advection-diffusion model (Schlüter et al., 2004), as shown in Eq. (4):

$$v\frac{\partial(\Phi C)}{\partial x} - D\frac{\partial^2(\Phi C)}{\partial x^2} = 0, \quad (4)$$

where C is the concentration of Cl^-, Φ is the porosity; D is the molecular diffusion coefficient of Cl^- in the sediment, x is depth, and v is the velocity. The Cl^- diffusion coefficient for sediment (D) was based on Boudreau (1997). The calculation included the measure of the average bottom-water temperature of each season: summer (17°C), autumn (7°C), spring (5.1°C), and winter (0.1°C). The obtained molecular diffusion coefficient was corrected for the effect of tortuosity (θ) according to Boudreau (1997), as shown in Eq. (5):

$$\theta^2 = 1 - \ln(\Phi^2). \quad (5)$$

The porosity was determined according to Bolałek (1992).

For Cl^- interpolation, the least-squares method was used, and the best function was obtained (Eq. (4)). The SGD velocity was then calculated as Eq. (6):

$$v = \frac{D\frac{\partial^2(\Phi C)}{\partial x^2}}{\frac{\partial(\Phi C)}{\partial x}}. \quad (6)$$

The SGD rate was calculated based on measures in every site and included: seasonal sampling in Swarzewo (4 pore water chloride profiles) and Chałupy (4 pore water chloride profiles); and single measure (1 pore water profile collected in July 2018) for each study site located in Hel, Jurata, Osłonino, and Puck.

The shallow sediments of the Bay of Puck are rapidly becoming hypoxic or anoxic with increasing sediment depth. Usually, there is no oxygen at approximately 2 cm below water-sediment interface (Szymczycha et al., 2012). Therefore in model assumptions, we neglected the bioturbation effect.

Salinity at the depth of 10 cm below water-sediment interface was measured in every sampling site (Fig. 2) while at the selected station within each site the pore water chloride profiles were taken (Fig. 3). These profiles enable to determine the SGD flux using the vertical, one-dimensional, advection-diffusion model. The calculated water flow was further extrapolated to the area where similar salinity was observed. To assign the area with similar salinity, the salinity surveys (Fig. 3) and CorelDRAW software were used. The portion of the area ranged from 5% to 25% (chapter 3.1). The literature denotes that approximately half of the Bay of Puck is under direct SGD influence (Kozerski (Ed.), 2007; Kryza and Kryza, 2006). Therefore, we assumed that SGD enters to the half of the Bay of Puck however the SGD fluxes obtained in this study are characteristic only of the assigned in this study area (from 5% to 25%). We simply extrapolated the obtained minimum and maximum flux to the area ranging from 9.1 km^2 to 45.5 km^2. Moreover, we did similar calculation and extrapolated the obtained results to the inner Bay of Puck.

2.6. Monitoring data

The wind speed and wind direction data were obtained from the Maritime Office in Gdynia, from automatic stations. The daily atmospheric precipitation data and mean sea level were obtained from the Institute of Meteorology and Water Management (IMGW) database (https://dane.imgw.pl/data) from land-based stations (IMGW, 2019). The data are presented in the supplementary material (Supplementary Material Tab. 1S and 2S). Data characterizing deep groundwater wells located at Hel, Jurata, and Puck (Fig. 1) and the Reda River were obtained from the Regional Inspectorate for Environmental Protection, 2019.

3. Results

3.1. Salinity and chloride distribution

Generally, average seawater salinity in the Bay of Puck oscillates around 7, and, usually, significantly lower surface water salinities indicate freshwater influence, such as that of rivers and/or precipitation. In terms of the pore water vertical distribution of salinity, the profiles are generally constant or increase slightly with depth (Carman and Rahm, 1997). The consistent presence of low salinity pore water designates SGD (Kotwicki et al., 2014; Pempkowiak et al., 2010; Schlüter et al., 2004; Szymczycha et al., 2012). Figure 2 presents the pore water salinity distributions at 10 cm depth in six sites within the Bay of Puck. Three of

Table 1 The macro ion concentrations in submarine groundwater discharge (SGD), shallow groundwater (piezometers), deep groundwater (groundwater wells), river (Reda River) and seawater.

Sample type		Average (mmol dm^{-3}) Range: min-max						
		Cl^-	HCO_3^-	SO_4^{2-}	Na^+	K^+	Ca^{2+}	Mg^{2+}
SGD	Nov 2017	39.8	0.88	0.12	31.5	1.54	2.3	5.9
		1.1–126.1	0.01–1.96	0.12–1.60	0.2–123.3	0.10–2.70	0.3–3.5	0.3–13.1
	Mar 2018	22.3	4.22	0.51	19.5	0.62	1.6	2.1
		1.1–116.8	2.17–9.11	0.10–1.60	0.2–81.6	0.10–2.40	0.3–2.6	0.3–9.9
	May 2018	25.4	0.47	0.13	30.1	1.19	2.0	4.1
		2.3–123.0	0.20–1.12	0.03–0.18	3.1–141.2	0.10–4.20	1.0–3.3	0.6–13.0
	Jul 2018	30.7	0.58	0.14	30.0	0.53	1.9	1.8
		1.4–109.0	0.04–1.33	0.03–0.35	1.9–127.0	0.20–1.20	1.0–3.7	0.4–6.2
Shallow groundwater		13.3	1.56	0.24	33.3	0.35	1.8	1.0
		1.1–58.4	0.04–9.11	0.03–1.24	0.2–99.3	0.10–0.80	0.3–3.3	0.3–3.9
Deep groundwater		1.0	2.60	0.30	1.2	0.10	0.8	0.25
		0.3–1.4	2.40–3.20	0.20–0.50	0.4–1.7	0.08–0.13	0.6–1.4	0.2–0.3
Seawater		143.2	1.12	0.14	128.6	2.50	2.7	7.9
		123.2–159.6	0.34–2.34	0.10–0.18	82.5–151.0	2.40–2.60	1.9–3.5	0.7–13.0
River		0.6	2.90	0.50	0.5	0.07	2.0	0.35
		0.4–0.9	2.50–3.30	0.40–0.60	0.4–0.6	0.06–0.08	1.9–2.1	0.3–0.4

the sites are located offHel Peninsula (a) Hel, (b) Jurata, (c) Chałupy, and the other three sites are situated offthe mainland (d) Swarzewo, (e) Puck, and (f) Osłonino (Fig. 1). All surveys indicate the high spatial variability of salinity distribution within each site, indicating that, in each case, a certain portion of sediment is influenced by direct SGD (salinity below 1 at 10 cm depth) at the time of sampling. The portion of the area with direct SGD impact ranged from 5% to 25%. However, in each case, only small portions of pore water (less than 10%) had salinities characteristic of seawater. The spatial variability of the pore water salinity distribution can be attributed to the movement of the groundwater-seawater mixing zone and, therefore, to variations in groundwater discharge rates and/or increase of freshwater salinity (Kaleris, 2018). The increase of freshwater salinity can be also caused by chloride aerosols derived from sea spray that enter the shallow groundwater with recharge (Pietrucień, 1983).

Figure 3 presents the seasonal pore water chloride profiles in (a) Swarzewo and (b) Chałupy. Additionally, the chloride vertical distribution obtained in July 2018 is presented for (c) all remaining sites. Chloride concentration decreased with increasing depth at every season and site. This pattern is typical of the Baltic Sea coast, which is influenced by fresh groundwater (Schlüter et al., 2004; Szymczycha et al., 2012). The presence of a seawater-dominated zone in the upper first 5 cm of the sediment was evidenced by high chloride concentrations, comparable to those of bottom-water (~143.2 mmol dm^{-3}). Below that layer, an occurrence of freshwater is indicated by chloride concentrations significantly decreasing, reaching 1.0 mmol dm^{-3}. A small spatial variability among chloride vertical distribution is visible. Interestingly, there was higher variability among seasons.

3.2. Macro ion composition

The macro ion compositions of SGD, shallow and deep groundwater, river water, and seawater in samples collected in 2017 and 2018 are listed in Table 1. Additionally, SGD samples are divided according to the time of sampling, while the other types of water represent the average, minimum, and maximum values obtained over the course of the study. The macro ion concentrations in SGD differ across seasons. Similar to SGD, high ranges of minimum and maximum concentrations of macro ions were also observed in seawater and shallow groundwater. The compositions of the Reda River and deep groundwater are stable, and no seasonal changes were observed.

The Piper diagram depicts the relative proportions of major ions on a charge-equivalent basis for comparison and classification of water samples independent of total analyte concentrations, and it is a graphical illustration of water chemistry. It is widely used in studies concerning the composition and origin of groundwater (Hounslow, 1995; Piper, 1994). Based on the major ion data, the chemical composition of collected water samples can be classified into several groups (Fig. 4). Seawater is a sodium-chloride (Na-Cl) type of water. River water is a calcium-bicarbonate type (Ca-HCO_3), and deep groundwater reflects a similar composition. Shallow groundwater (samples from piezometers), depending on the season, is a Ca-HCO_3 type of water (in the summer (July 2018) and winter (March 2018)) or a Na-Cl type of water (in autumn (November 2017) and spring (May 2018)). SGD samples are generally Na-Cl types, showing the great influence of seawater intrusion.

Transformations in water chemistry can be reflected by flow paths presented as a series of points along trend lines in Fig. 4. Samples near the straight line (F-S) represent

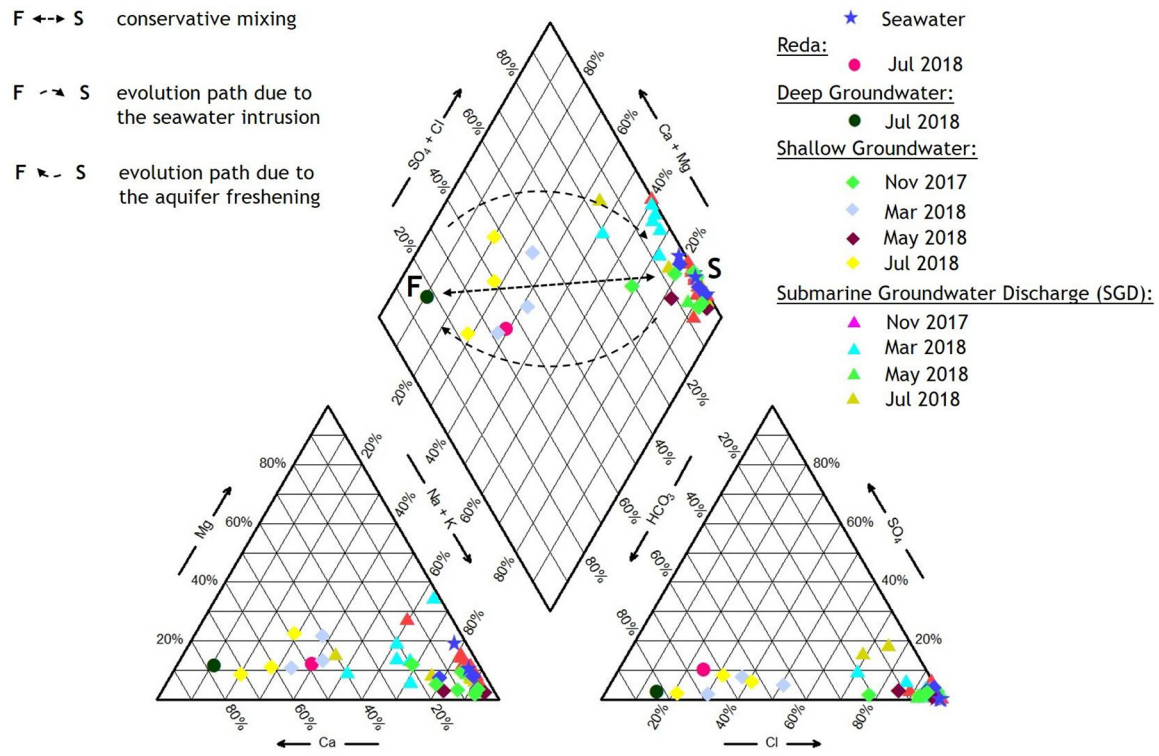

Figure 4 Piper diagram showing the ionic composition (% meq dm^{-3}) of seawater (seawater endmember), river water (Reda River, monitoring data), deep (monitoring data) and shallow groundwater, and submarine groundwater discharge (SGD). Samples of shallow groundwater and SGD were collected seasonally. The conservative (straight broken line) and nonconservative (concave and convex broken line) mixing between freshwater (F) and seawater (S) end-members are shown.

a mixture between the seawater (S) and freshwater (F) end-members. The upper path shows the direction along which the freshwater is replaced by seawater while the upward paths present the opposite process. In our data sets, no clear trends were observed. Samples from groundwater wells and the river were located generally closer to the upward evolution path denoting the aquifer freshening while SGD samples depending on the season showed both trends. It seems that in March and November the composition of most of the SGD samples was under higher seawater influence while in May and July the composition moved towards freshwater.

Groundwater often contains dissolved calcium, or magnesium, which originate from the weathering of surface rocks as well as dissolved organic compounds such as detritus, animal waste, or human contaminants. Since this water percolates through an aquifer, it may be modified and changed. Groundwater and accompanied dissolved calcium or magnesium moves towards the sea. Eventually, these ions may be exchanged for sodium in groundwater-seawater mixing zone and might form salts (Liu et al., 2017; Salem et al., 2016). The relationship between ΔMg^{2+}, ΔCa^{2+}, and $(\Delta Na^{+} + \Delta K^{+})$ is presented in Fig. 5. The collected water samples characterizing the coastal area can be divided into several zones according to the ionic deltas of cations (Liu et al., 2017). Each zone is represented as a quadrant from I to IV. At the direction from dissolution (I) to precipitation (III), the external sources or sinks play a key role in controlling the concentration of ions in the water. The other direction represents the cation exchange (II and IV). In quadrant II, Mg^{2+} or Ca^{2+} is exchanged with Na^{+} and K^{+}, and, in quadrant IV, the process is the opposite (Liu et al., 2017). The ionic deltas (ΔMg^{2+}, ΔCa^{2+}, and $(\Delta Na^{+} + \Delta K^{+})$) of collected samples mainly indicate the dissolution and cation exchange processes. The possible precipitation of magnesium and calcium was observed in only few samples collected in Mar and May 2018. Both positive ΔMg^{2+} and ΔCa^{2+} concentrations and positive $(\Delta Na^{+} + \Delta K^{+})$ and the Mg^{2+}/Ca^{2+} ratio lower than 0.5, show a possible dissolution of calcite mainly in Nov 2017 and Jul 2018. The possible cation exchange process was most pronounced in May 2017. Both processes namely the dissolution and cation exchange imply the dynamic processes that occur in the groundwater seawater mixing zone.

4. Discussion

4.1. SGD flux to study sites

The obtained chloride pore water profiles can deliver information about fluid transport in sediments (Schlüter et al., 2004). Hence, diffusion is indicated by a linear decrease in the Cl^{-} concentration, while the freshwater flow is indicated by a concave-shaped curve (Oehler et al., 2017; Schlüter et al., 2004). In this study, the pore water chloride profiles had the concave shape indicative of freshwater flow. Therefore, to estimate the SGD rate, we used a

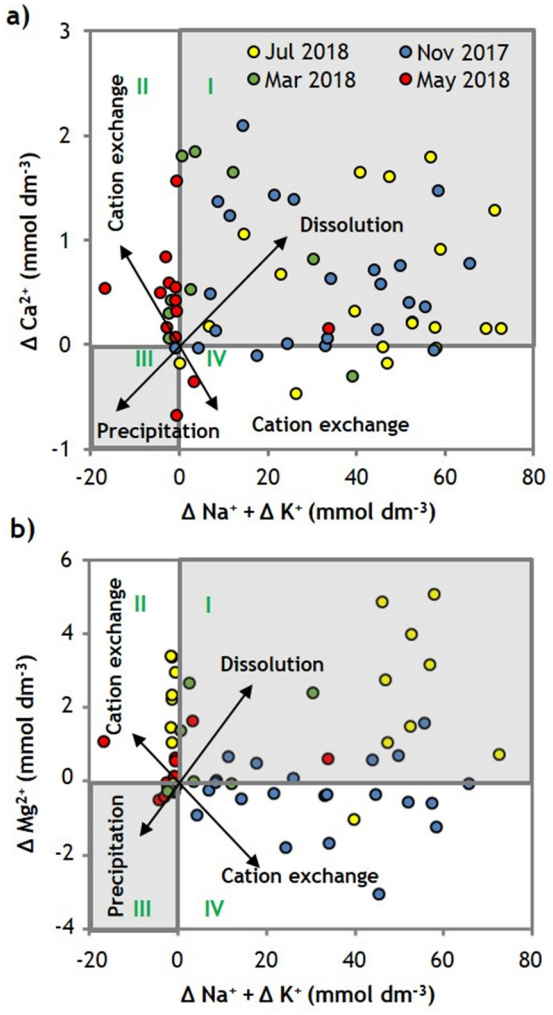

Figure 5 The ΔMg^{2+} and ΔCa^{2+} (mmol dm^{-3}) are plotted vs. ($\Delta Na^{+}+\Delta K^{+}$) (mmol dm^{-3}) for each sample to reveal the mechanism of enrichment or depletion of major cations in the mixing zone (transition zone = subterranean estuary) of the Bay of Puck. The quadrants from I to IV indicate several processes such as: dissolution (I), cation exchange (II and IV), and precipitation (III).

one-dimensional, advection-diffusion model based on the vertical chloride distribution (12 chloride pore water profiles presented at Fig. 3). The functions used for calculations are listed in the Supplementary Material Tab. 1S while the obtained fluxes are shown in Table 2. Surprisingly there was no significant spatial variability among sites in calculated SGD rates. The pronounced seasonal changes are visible, with the highest flux observed in July 2018 and the lowest in November 2017 and May 2018. The seasonal SGD flux variability was also observed in previous studies located off Hel (Szymczycha et al., 2012). The SGD flux to the Bay of Puck obtained in this study was comparable with seepage rates (Szymczycha et al., 2012) but was significantly lower (several orders of magnitude) than groundwater flux estimated by means of gradient meter method (Bublijewska et al., 2017). In the Eckernförde Bay, Western Baltic Sea SGD flux was estimated using similar to this study approach and the calculated flux was two orders of magnitude lower than

Table 2 The SGD flux measured in Chałupy, Swarzewo, Jurata, Hel, Swarzewo, Puck, and Osłonino.

Date	SGD in each study area (x 10^{-7} L cm^{-2} s^{-1})					
	Chałupy	Jurata	Hel	Swarzewo	Puck	Osłonino
Nov 2017	1.8	nd	nd	1.8	nd	nd
Mar 2018	2.3	nd	nd	2.2	nd	nd
May 2018	1.8	nd	nd	1.8	nd	nd
Jul 2018	2.7	2.6	2.7	2.8	2.0	2.8

nd — no data.

submarine groundwater discharge to the Bay of Puck. One reason for that can be difference in hydrogeological characteristics of both bays.

SGD is influenced by the components of the short-timescale (minutes, hours, days) which are due to wave actions, tides, and precipitation as well as the components of the long-timescale — which result from the seasonal movement of the mixing zone and large-scale, sea level variations (Kaleris, 2018). SGD was correlated with average speed, the direction of the wind, and the total precipitation within 72 h prior sampling (Supplementary Material Tab. 2S) and with the total monthly precipitation and sea level change (Supplementary Material Tab. 3S). The 72 h (h) time interval was based on Kozerski (Ed.) (2007), who estimated the shallow groundwater residence time to be 72 h in the Bay of Gdańsk region. In this study, the wind speed ranged from 2.9 m s^{-1} to 4.6 m s^{-1} and did not correlate with increased or decreased SGD fluxes (Tab. 2S). Reversely, a correlation of increased SGD flux and increased total precipitation within 72 h prior sampling was observed (Supplementary Material Tab. 2S). Generally, in November 2017 the total precipitation (Supplementary Material Tab. 3S) was highly similar to the sea level. In March 2018, the sea level significantly decreased, while the precipitation rate was at an average magnitude. In May 2018, the wind changed direction to the northeast (Supplementary Material Tab. 3S), and the sea level started to increase while the average monthly precipitation and total precipitation stayed at an average rate. In July 2018, the south wind direction was observed, total precipitation slightly increased while no significant increase in sea level was observed. It seems that increased precipitation increases SGD rate if there is no rise in sea level. In addition, south wind can move the seawater from the southern coast further seaward and can enable groundwater to discharge more even if the precipitation is at an average rate. The wind direction at the time before and during sampling, average monthly precipitation, and sea level conditions significantly influenced the SGD rate, while wind speed several hours prior to sampling was less important. It seems that all three drivers (wind direction at the time before and during sampling, precipitation, and sea level conditions) can be used as parameters enabling the estimation of the SGD rate change.

4.2. SGD flux to the Bay of Puck

Several studies have concentrated on SGD along the coastal areas of the Baltic Sea (e.g., Kozerski (Ed.), 2007; Kryza

Table 3 Extrapolated SGD fluxes.

Date	Extrapolated SGD to the Bay of Puck based on salinity distribution and assuming that half of the bay is under SGD influence min–max ($m^3\ s^{-1}$)	Extrapolated SGD to the inner Bay of Puck based on salinity distribution and assuming half of the bay is under SGD influence min–max ($m^3\ s^{-1}$)
Nov 2017	16.4–82.1	9.2–47.3
Mar 2018	20.2–101.1	11.7–58.7
May 2018	16.3–80.1	9.4–46.1
Jul 2018	24.8–127.7	14.3–73.5
Annually	16.3–127.7	9.2–73.5

and Kryza, 2006; Peltonen 2002; Piekarek-Jankowska 1994; Viventsowa and Voronow, 2003) mostly addressing the fresh component of SGD. The magnitude of SGD was negligible in comparison to river runoff. Consequently, the scientific community has recognized SGD (both fresh SGD and recirculated SGD) as an insignificant factor affecting the ecosystem of the Baltic Sea. It is worth noticing that in the global literature, we can find results indicating that seawater circulation caused by tide and wave set-up may contribute 96% of the total SGD compared to 4% of fresh SGD (Li et al., 1999). Interestingly, Krall et al. (2017) indicated that SGD rates at Forsmark, Gulf of Bothnia, Baltic Sea are significantly higher than results obtained from local hydrological models, which consider only the fresh component of SGD.

Given the absence of SGD flux to the Bay of Puck including the fresh and recirculated SGD we extrapolated the results obtained in each study site to the entire bay. The details related to the extrapolation methodology are given in the materials and methods chapter. The obtained SGD flux to the entire Bay of Puck ranged from 16.0 $m^3\ s^{-1}$ to 127.7 $m^3\ s^{-1}$ while to the inner Bay of Puck ranged from 9.2 $m^3\ s^{-1}$ to 73.5 $m^3\ s^{-1}$ (Table 3). The wide range of obtained flux can be due to the seasonal variability of SGD. The obtained result is significantly higher than the fresh SGD flux calculated by Piekarek-Jankowska (1994). Moreover, it is from 2.5 to 25 times more than the annual discharge of the biggest river entering the Bay of Puck – the Reda River (5 $m^3\ s^{-1}$). Matciak et al. (2015) seem to confirm our results. They observed salinity anomalies in the bottom-water of the Bay of Puck and suggested that less saline water appeared and changed the seawater salinity. The volume of freshwater must have been significant to reduce the bottom-water salinity. In comparison to other sites located in the Baltic Sea, the SGD fluxes to the Bay of Puck are notably higher (Schlüter et al., 2004). Recently, Krall et al. (2017) indicated, on the basis of a ^{224}Ra mass balance, that SGD rate at Forsmark, Gulf of Bothnia, Baltic Sea ranges from $(5.5 \pm 3.0) \times 10^3\ m^3\ d^{-1}$ to $(950 \pm 520) \times 10^3 m^3\ d^{-1}$. These rates are up to three orders of magnitude lower than those obtained during this study. The significant differences in estimated SGD rates can be related to both (1) different hydrogeological characteristics of both sites and (2) different method used to calculated SGD flux.

We are aware that the extrapolated SGD involves errors and uncertainties. However, we wanted to show the order of magnitude rather than the actual numbers. SGD is a source of chemical substances globally (Cai et al., 2003; Charette and Sholkovitz, 2002, 2006; Kroeger et al., 2007), and, certainly, it supplies the Bay of Puck with nutrients or dissolved carbon (Szymczycha et al., 2012, 2014). Therefore, it should be considered as a driver for ecosystem change, such as algae blooms and eutrophication. We would like to encourage the scientific community to acknowledge SGD as a significant source of water and, most probably, an important source of chemical substances. The future SGD studies in the Baltic Sea region should include the similar approach to estimate SGD, and, additionally, include several different methods such as analytical or numerical modeling; direct measurements; and environmental tracer techniques.

5. Conclusions

SGD in the Bay of Puck ranged from 16.0 $m^3\ s^{-1}$ to 127.7 $m^3\ s^{-1}$, which is significantly higher than previously obtained results by Piekarek-Jankowska (1994) that excluded the recirculated seawater component of SGD. The flux obtained in this study correlates well with the observations of the bottom water salinity anomalies in the Bay of Puck (Matciak et al., 2015). The SGD rate and its' composition correlated with both short-time scale factors (wind direction and precipitation) and long-timescale factors (seasonal movement of the mixing zone and large-scale sea level variations).

This study demonstrates a need to include SGD as a source of water and, most probably, chemical substances in studies characterizing the functioning of the coastal areas of the Baltic Sea. In order to better understand the generation and fate of SGD in the Bay of Puck and other Baltic Sea coastal areas, further studies are needed.

Acknowledgments

The results reported herein were obtained within the framework of the statutory activities of the Institute of Oceanology Polish Academy of Sciences and the following research projects: PharmSeepage 2016/21/B/ST10/01213, funded by the Polish National Science Center, and WaterPUCK BIOSTRATEG3/343927/3/NCBR/2017, financed by the National

Center for Research and Development (NCBiR) within the BIOSTRATEG III program.

We thank Leszek Łęczyński, Emilia Bublijewska, and Marcin Stokowski for their help in installing piezometers. We are also grateful to Tadeusz Ossowski for help in enabling the laboratory facilities in order to analyze chloride, bicarbonates, and sulphates in water samples. We thank Jolanta Walkusz-Miotk for help in major cations analyses. We thank the anonymous reviewers for their careful reading of our manuscript and their many insightful comments and suggestions.

Supplementary materials

Supplementary material associated with this article can be found, in the online version, at doi:10.1016/j.oceano.2019.09.001.

References

Appelo, C., Postma, D., 2005. Geochemistry, Groundwater and Pollution, 2nd edn. Balkema, Rotterdam, 683 pp., http://dx.doi.org/10.1201/9781439833544.

Bolałek, J., 1992. Ionic macrocomponents of the interstitial waters of Puck Bay sediments. Oceanologia 33, 131—158.

Boudreau, B.P., 1997. Diagenetic Models and Their implementation: Modelling Transport and Reactions in Aquatic Sediments. Springer—Verlag, Berlin, Heidelberg, New York, 414 pp.

Bublijewska, E., Łęczyński, L., Marciniak, M., Chudziak, Ł., Kłostowska, Ż., Zarzeczańska, D., 2017. In situ measurements of submarine groundwater supply from the Puck Lagoon. Prz. Geol. 65 (11—2), 1173—1178.

Burnett, W.C., Bokuniewicz, H., Huettel, M., Moore, W.S., Taniguchi, M., 2003. Groundwater and pore water inputs to the coastal zone. Biogeochemistry 66 (1—2), 3—33, https://doi.org/10.1023/B:BIOG.0000006066.21240.53.

Burnett, W.C., Aggarwal, P.K., Aureli, A., Bokuniewicz, H., Cable, J.E., Charette, M.A., Kontar, E., Krupa, S., Kulkarni, K.M., Loveless, A., Moore, W.S., Oberdorfer, J.A., Oliveira, J., Ozyurt, N., Povinec, P., Privitera, A.M.G., Rajar, R., Ramessur, R.T., Scholten, J., Stieglitz, T., Taniguchi, M., Turner, J.V., 2006. Quantifying submarine groundwater discharge in the coastal zone via multiple methods. Sci. Total Environ. 367 (2—3), 498—543, https://doi.org/10.1016/j.scitotenv.2006.05.009.

Cai, W.—J., Wang, Y.—C., Krest, J., Moore, W.S., 2003. The geochemistry of dissolved inorganic carbon in a surficial groundwater aquifer in North Inlet, South Carolina, and the carbon fluxes to the coastal ocean. Geochim. Cosmochim. Ac. 67 (4), 631—639, https://doi.org/10.1016/S0016-7037(02)01167-5.

Carman, R., Rahm, L., 1997. Early diagenesis and chemical characteristics of interstitial water and sediments in the deep deposition bottoms of the Baltic proper. J. Sea Res. 37 (1—2), 25—47, https://doi.org/10.1016/S1385—1101(96)00003—2.

Charette, M.A., Sholkovitz, E.R., 2002. Oxidative precipitation of groundwater—derived ferrous iron in the subterranean estuary of a coastal bay. Geophys. Res. Lett. 29 (10), 85—1—85—4, https://doi.org/10.1029/2001GL014512.

Charette, M.A., Sholkovitz, E.R., 2006. Trace element cycling in a subterranean estuary: part 2. Geochemistry of the pore water. Geochim. Cosmochim. Ac. 70 (40), 811—826, https://doi.org/10.1016/j.gca.2005.10.019.

Cyberski, J., 1993. Hydrologia zlewiska. In: Korzeniewski, K. (Ed.), Zatoka Pucka. Fundacja Rozwoju Uniwersytetu Gdańskiego, Gdańsk, 40—70.

Hounslow, A.W., 1995. Water Quality Data: Analysis and Interpretation. CRC Press LLC, Lewis Publishers, Boca Raton, 416 pp., https://doi.org/10.1201/9780203734117.

Institute of Meteorology and Water Management (IMGW) database, https://dane.imgw.pl/data, (accessed on 21.08.2019).

Jiao, J., Post, V., 2019. Coastal Hydrogeology. Cambridge University Press, Cambridge, 404 pp., https://doi.org/10.1017/9781139344142.

Kaleris, V., 2018. Submarine groundwater discharge and its influence on the coastal environment. Available from: http://www.coastalwiki.org/wiki/Submarine_groundwater_discharge_and_its_influence_on_the_coastal_environment, (accessed on 20—08—2019).

Kotwicki, L., Grzelak, K., Czub, M., Dellwig, O., Gentz, T., Szymczycha, B., Böttcher, M.E., 2014. Submarine groundwater discharge to the Baltic coastal zone: impacts on the meiofaunal community. J. Marine Syst. 129, 118—126, https://doi.org/10.1016/j.jmarsys.2013.06.009.

Kozerski, B., 2007. In: Jaworska—Szulc, B., Piekarek—Jankowska, H., Pruszkowska, M., Przewłócka, M. (Eds.), Gdański System Wodonośny. Wydawnictwo Politechniki Gdańskiej, Gdańsk, 113 pp.

Krall, L., Trezzi, G., Garcia—Orellana, J., Rodellas, V., Morth, C.—M., Andersson, M., 2017. Submarine groundwater discharge at Forsmark, Gulf of Bothnia, provided by Ra isotopes. Mar. Chem. 196, 162—172, https://doi.org/10.1016/j.marchem.2017.09.003.

Kroeger, K.D., Swarzenski, P.W., Greenwood, J.Wm., Reich, C., 2007. Submarine groundwater discharge to Tampa Bay: nutrient fluxes and biogeochemistry of the coastal aquifer. Mar. Chem. 104 (1—2), 85—97, https://doi.org/10.1016/j.marchem.2006.10.012.

Kryza, J., Kryza, H., Pruszkowska, M., Szczepiński, J., Szlufik, A., Tomaszewski, B., 2005. Dokumentacja hydrogeologiczna określająca warunki bezpośredniego odpływu podziemnego do akwenu bałtyckiego z analizą możliwości zagospodarowania i ochrony wód podziemnych. Integrated Management Services, Wrocław, 138 pp.

Kryza, J., Kryza, H., 2006. The analytic and model estimation of the direct groundwater flow to Baltic sea on the territory of Poland. Geologos 10, 153—166.

Li, L., Barry, D.A., Stagnitti, F., Parlange, J.—Y., 1999. Submarine groundwater discharge and associated chemical input to a coastal sea. Water Resour. Res. 35 (11), 3253—3259, https://doi.org/10.1029/1999WR900189.

Liu, Y., Jiao, J.J., Liang, W., Kuang, X., 2017. Hydrogeochemical characteristics in coastal groundwater mixing zone. Appl. Geochem. 85 (Pt. A), 49—60, https://doi.org/10.1016/j.apgeochem.2017.09.002.

Matciak, M., Bieleninik, S., Botur, A., Podgórski, M., Trzcińska, K., Dragańska, K., Jaśniewicz, D., Kurszewska, A., Wenta, M., 2015. Observations of presumable groundwater seepage occurrence in Puck Bay (the Baltic sea). Oceanol. Hydrobiol. St. 44 (2), 267—272, https://doi.org/10.1515/ohs—2015—0025.

Moore, W.S., 1996. Large groundwater inputs to coastal waters revealed by 226Ra enrichments. Nature 380, 612—614, https://doi.org/10.1038/380612a0.

Moore, W.S., 2010. The effect of submarine groundwater discharge on the ocean. Annu. Rev. Mar. Sci. 2 (1), 59—88, https://doi.org/10.1146/annurev—marine—120308—081019.

Nowacki, J., 1993. Morfometria zatoki. In: Korzeniewski, K. (Ed.), Zatoka Pucka. Inst. Oceanogr., UG, Gdańsk, 71—78.

Oehler, T., Mogollón, J.M., Moosdorf, N., Winkler, A., Kopf, A., Pichler, T., 2017. Submarine groundwater discharge within a landslide scar at the French Mediterranean coast. Estuar. Coast. Shelf Sci. 198, 128—137, http://dx.doi.org/10.1016/j.ecss.2017.09.006.

Peltonen, K., 2002. Direct Groundwater Inflow to the Baltic Sea. TemaNord, Nordic Councils of Ministers, Copenhagen, Netherlands, 79 pp.

Pempkowiak, J., Szymczycha, B., Kotwicki, L., 2010. Submarine groundwater discharge (SGD) to the Baltic Sea. Rocz. Ochr. Środ. 12 (1), 17—32.

Piekarek—Jankowska, H., Łęczyński, L., 1993. Morfologia dna. In: Korzeniewski, K. (Ed.), Zatoka Pucka. Fundacja Rozwoju UG, Gdańsk, 222—281.

Piekarek—Jankowska, H., 1994. Zatoka Pucka jako Obszar Drenażu Wód Podziemnych. Rozp. Monogr. 204, Wyd., UG, Gdańsk, 31—32.

Piekarek—Jankowska, H., 1996. Hydrochemical effects of submarine groundwater discharge to the Puck Bay (southern Baltic Sea, Poland). Geographica Polonica 67, 103—119.

Pietrucień, Cz., 1983. Regionalne Zróżnicowanie Warunków Dynamicznych i Hydrochemicznych Wód Podziemnych w Strefie Brzegowej Południowego i Wschodniego Bałtyku. Wyd. UMK, Toruń, 269 pp.

Piper, A.M., 1994. A graphic procedure in the geochemical interpretation of water analysis. Am. Geophys. Union Trans. 25, 914—923.

Regional Inspectorate for Environmental Protection (http://www.gios.gov.pl/pl/, (accessed on 21.08.2019).

Salem, Z.E., Al Temamy, A.M., Salah, M.K., Kassab, M., 2016. Origin and characteristics of brackish groundwater in Abu Madi coastal area, Northern Nile Delta, Egypt. Estuar. Coast. Shelf Sci. 178, 21—35, https://doi.org/10.1016/j.ecss.2016.05.015.

Santos, I.R., Burnett, W.C., Chanton, J., Mwashote, B., Suryaputra, I.G.N.A., Dittmar, T., 2008. Nutrient biogeochemistry in a Gulf of Mexico subterranean estuary and groundwater—derived fluxes to the coastal ocean. Limnol. Oceanogr. 53 (2), 705—718, https://doi.org/10.4319/lo.2008.53.2.0705.

Schlüter, M., Sauter, E.J., Andersen, C.E., Dahlgaard, H., Dando, P.R., 2004. Spatial distribution and budget for submarine groundwater discharge in Eckernförde Bay (Western Baltic Sea). Limnol. Oceanogr. 49 (1), 157—167, https://doi.org/10.4319/lo.2004.49.1.0157.

Szymczycha, B., Vogler, S., Pempkowiak, J., 2012. Nutrient fluxes via submarine groundwater discharge to the Bay of Puck, southern Baltic Sea. Sci. Total Environ. 438, 86—93, https://doi.org/10.1016/j.scitotenv.2012.08.058.

Szymczycha, B., Maciejewska, A., Winogradow, A., Pempkowiak, J., 2014. Could submarine groundwater discharge be a significant carbon source to the southern Baltic Sea? Oceanologia 56 (2), 327—347, https://doi.org/10.5697/oc.56—2.327.

Szymczycha, B., Kroeger, K.D., Pempkowiak, J., 2016. Significance of groundwater discharge along the coast of Poland as a source of dissolved metals to the southern Baltic Sea. Mar. Pollut. Bull. 109 (1), 151—162, https://doi.org/10.1016/j.marpolbul.2016.06.008.

Urbański, J., Grusza, G., Chlebus, N., 2007. Fizyczna Typologia Dna Zatoki Gdańskiej. Pracownia Geoinformacji Zakładu Oceanografii Fizycznej. Instytut Oceanografii UG, Gdynia, 8 pp.

Uścinowicz, S., Kramarska, R., 2011. Geological setting and bottom sediments in the Baltic Sea. The quaternary basement. In: Uścinowicz, S. (Ed.), Geochemistry of Baltic Sea Surface Sediments. Pol. Geol. Inst. — Nat. Res. Inst., 66—70.

Viventsowa, E.A., Voronow, A.N., 2003. Groundwater discharge to the Gulf of Finland (Baltic Sea): ecological aspects. Environ. Ecol. 45, 221—225.